

Experimental investigation of the effect of vegetation on dam break flood waves

Semire Oguzhan, Aysegul Ozgenc Aksoy*

Department of Civil Engineering, Dokuz Eylul University, Tinaztepe Campus, 35160, Buca, Izmir, Turkey.

* Corresponding author. Tel.: 0090-232-3017019. E-mail: aysegul.ozgenc@deu.edu.tr

Abstract: Dams have an important role in the industrial development of countries. Irrespective of the reason for dam break, the flood can cause devastating disasters with loss of life and property especially in densely populated areas. In this study, the effects of the vegetation on the flood wave propagation in case of dam break were investigated experimentally by using the distorted physical model of Ürkmez Dam. The horizontal and vertical scales of the distorted physical model are 1/150 and 1/30, respectively. The dam break scenarios were achieved by means of a gate of rectangular and triangular shape. The results obtained from experiments performed with vegetation were compared and interpreted with those obtained from experiments at which the vegetation configuration was absent. The analysis of the experimental data showed that the presence of vegetation causes a significant decrease in water depths as the flood wave propagates to the downstream and greatly reduces its impact on the settlements. It is also revealed that dam break shape plays an important role in temporal variation of flood wave.

Keywords: Dam break; Flood wave; Physical model; Ürkmez Dam; Vegetation effect.

1 INTRODUCTION

Dams are constructed for agricultural irrigation, drinking water supply, flood prevention and energy generation purposes. Dams have an important role in the economic development of countries. Irrespective of the reason of the dam break the flood can cause devastating disasters with loss of life and property especially in densely populated areas. The time required to warn people living in the downstream portion of the dam is very short in the case of floods resulting from a dam break. The most important reasons for the failure of earth dams are overtopping, piping and dam foundation problems. There are many references in the literature to dam break modeling. Investigations of the flood propagation will be also useful for emergency action plans.

Most of the dam break experiments have been carried out to investigate flood wave propagation. Lauber and Hager (1998) investigated the dam collapse in a horizontal rectangular channel with a length of 14 m and a width of 0.5 m. Wave velocities and water surface profiles were determined by means of particle image velocimetry and camera images, respectively. Soares-Frazão (2007) examined the flood wave propagation as a result of the collapse of the dam in a rectangular channel 5.6 m long and 0.5 m wide. The water depths were measured by means of water level gauges and digital camera. Soares-Frazão and Zech (2008) investigated the effect of flood waves on residential areas experimentally and numerically. The experiments were performed in a 36 m long and 3.6 m wide rectangular channel. The measured water depths and velocities were compared with those obtained from the numerical analysis. Ferrari et al. (2010) studied flood wave propagation on a plane dry bottom after a dam break. Two different mathematical models were established and the results were compared with those obtained by the experimental study. Ozmen-Cagatay and Kocaman (2010) investigated dam break flows in a rectangular channel with a horizontal smooth bed. In this study, Reynolds-average Navier-Stokes (RANS) equations combined with a $k-\epsilon$ turbulence model and the shallow water equation (SWE) were solved by

using the FLOW-3D software. The numerical results were compared with experimental data. They result of both models agreed well with the experimental results. Ismail et al. (2012) experimentally investigated the effect of a forest on a tsunami wave. The experiments were carried out in a rectangular channel 16.6 m long, 0.92 m wide and 0.7 m high. They created a flood wave by opening of the gate. LaRocque et al. (2013) carried out dam break experiments by means of an experimental setup that is 7.31 m long, 0.18 m wide and 0.42 m high. The experiments were performed for three different upstream heads. The Fluent software package was used to simulate the experimental system; the numerical results were compared with the experimental findings. Güney et al. (2014) investigated flood wave propagation experimentally by means of a distorted physical model of the Ürkmez Dam located close to Izmir, Turkey. The distorted model has a horizontal scale of 1/150 and a vertical scale of 1/30, including dam reservoir and downstream area. The sudden partial dam break was simulated by a trapezoidal breach located on the dam body. Water levels and velocities were measured at several locations in the downstream area of the model. Ozmen-Cagatay et al. (2014) and Kocaman and Ozmen-Cagatay (2015) investigated dam break floods and shock waves experimentally and numerically. The experiments were performed in a horizontal rectangular flume of 8.90 m in length, 0.30 m in width, and 0.34 m in height. The numerical simulations were carried out using the Flow-3D software package. The experimental results were compared to those obtained from the numerical simulation. He et al. (2017) investigated a depth-averaged 2D model for dam-break flows over mobile and vegetated beds. Laboratory results were used to validate the numerical studies. Haltas et al. (2016) investigated the flood inundation following the failure of the Ürkmez Dam. HEC-RAS and FLO-2D packages were used to simulate the flood propagation. Zhang et al. (2016) investigated dam-break wave processes by means of a depth-averaged 2-D model considering the sediment transport and the bed variation. Elkholy et al. (2016) investigated partial-breach dam-break flow experimentally. This was performed in a large basin including an up-

stream reservoir and a downstream basin. The upstream reservoir was 4.3 m wide, 3m long, and could be filled with water up to 0.75 m depth. The downstream basin was 8 m long and 4.3 m wide. During the experiments, three different initial upstream water depths were considered. Zhang et al. (2017) investigated 3D numerical modelling of dam-break flow hydrodynamics in an open L-shaped channel. The numerical results were compared with the experimental data and good agreement has been achieved between numerical and experimental results. Hooshyaripor et al. (2017) examined the effect of different reservoir capacities and side slopes on the flood wave propagation. The experimental setup had an upstream reservoir with a length of 4.5 m and a width of 2.25 m and downstream area 9.3 m long, 0.51 m wide and 0.7 m high. During the experiments, the time series of water level and velocity were recorded at several locations of the reservoir and downstream area. Liu et al. (2018) investigated the impact of dam failure on buildings by conducting experimental studies on a physical model of a house. The experiments were conducted in a horizontal flume with a length of 40 m, a width of 3.5 m and a depth of 0.4 m. The flood wave propagation was generated by quickly lifting up the gate. The prototype scale of the house was 8 m in width, 4 m in depth, and 6 m in height. The model house was geometrically undistorted. The water-level data were measured by means of pressure gauges and ultrasonic wave gauges.

According to the literature review the flood wave propagation as a result of dam break were generally investigated by conducting flume experiments. There are very few physical model experiments in the literature. In this study, the effects of vegetation on the flood wave propagation due to a dam break were investigated experimentally by using distorted physical model of the Urkmez Dam. The horizontal and vertical scales of the distorted physical model were 1/150 and 1/30, respectively. The resulting water level and velocity values were compared with those obtained from experiments of Tayfur et al. (2013) in which the vegetation configuration was not considered.

2 MATERIALS AND METHODS

2.1 Distorted physical model

The flood wave propagation of dam break by means of rectangular and triangular breaches were investigated experimentally by using the distorted physical model of Urkmez Dam. The horizontal and vertical scales of the distorted physical model are $L_{r,x} = 1/150$ and $L_{r,z} = 1/30$, respectively. The distorted model includes Urkmez Dam Lake and its downstream residential area. The experiments were performed by using the distorted physical model that was designed and constructed in the Hydraulic Laboratory of Civil Engineering Department within the Dokuz Eylul University. The design and construction details of the distorted physical model were given by Guney et al. (2014).

For the Froude model simulation

$$T_r = \frac{T_m}{T_p} = \frac{L_{r,x}}{\sqrt{L_{r,z}}} = \frac{1}{m_d} L_{r,z}^{1/2} \quad (1)$$

$$V_r = \frac{L_{r,x} m_d}{L_{r,z}^{1/2}} \quad V_r = V_m / V_p \quad (2)$$

where T_r is the time ratio, T_m the time in the physical model, T_p the time in the prototype, V_r the velocity ratio, V_m the velocity in the physical model, V_p the velocity in the prototype and

$m_d (= L_{r,z} / L_{r,x})$ the distortion coefficient. The characteristics of the prototype and physical model are given in Table 1.

Table 1. Characteristics of prototype and physical model.

Characteristic	Prototype	Model
Height of dam (m)	32	1.07
Crest length (m)	426	2.84
Crest width (m)	12	0.08
Reservoir volume for minimum level (m ³)	375000	0.556
Reservoir volume for maximum level (m ³)	8625000	12.78
Reservoir volume for normal level (m ³)	7950000	11.78
Active capacity (m ³)	7575000	11.22

Unlike previous studies, the vegetation configuration was incorporated into the downstream part of the Urkmez dam physical model using satellite images and field work. The vegetation configuration, simulated by plastic brushes, was located by taking into consideration the model scales. Hence all of the components of roughness were included in the model. Images of the physical model without and with vegetation are given in Figure 1.



Fig. 1. Physical model of Urkmez Dam Lake and downstream region without vegetation and with vegetation.

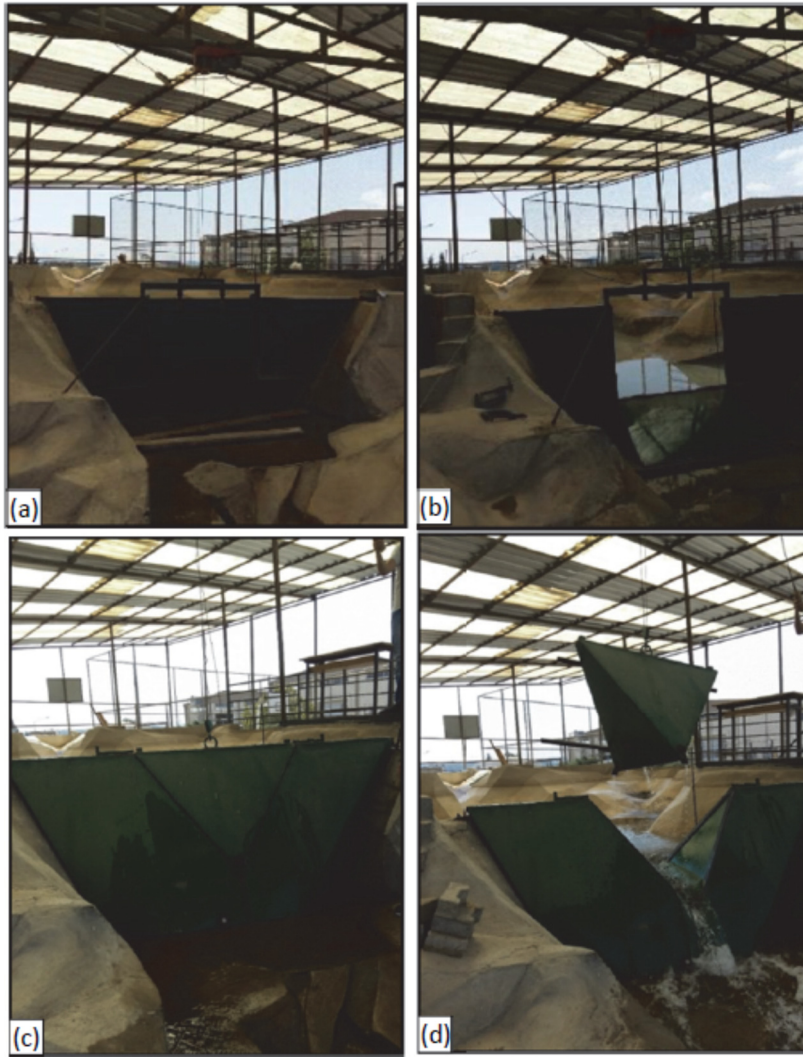
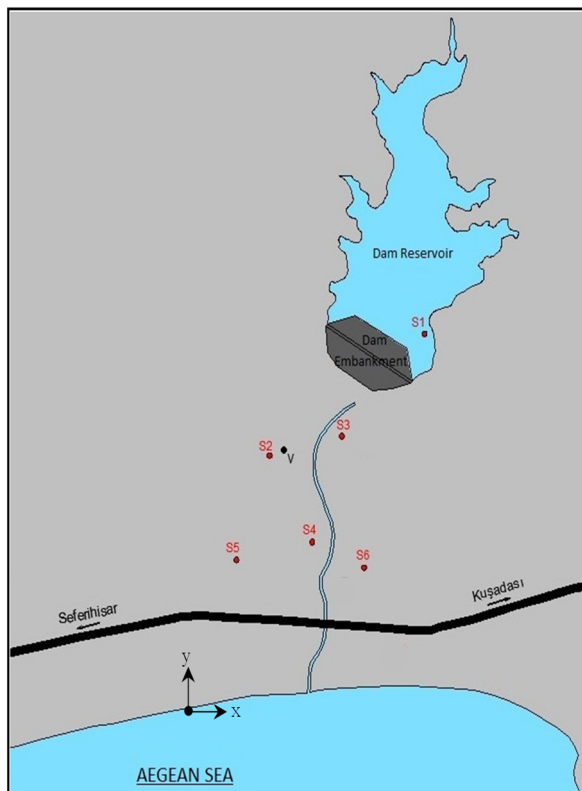


Fig. 2. Dam break mechanisms a)–b) Rectangular shape c)–d) Triangular shape.



Measurement point	X (m)	Y (m)
V	3.81	11.45
S2	3.75	11.4
S3	4.78	12.42
S4	3.8	8.04
S5	0.53	7.93
S6	6.93	6.72

Fig. 3. Locations of measurement points on physical model.

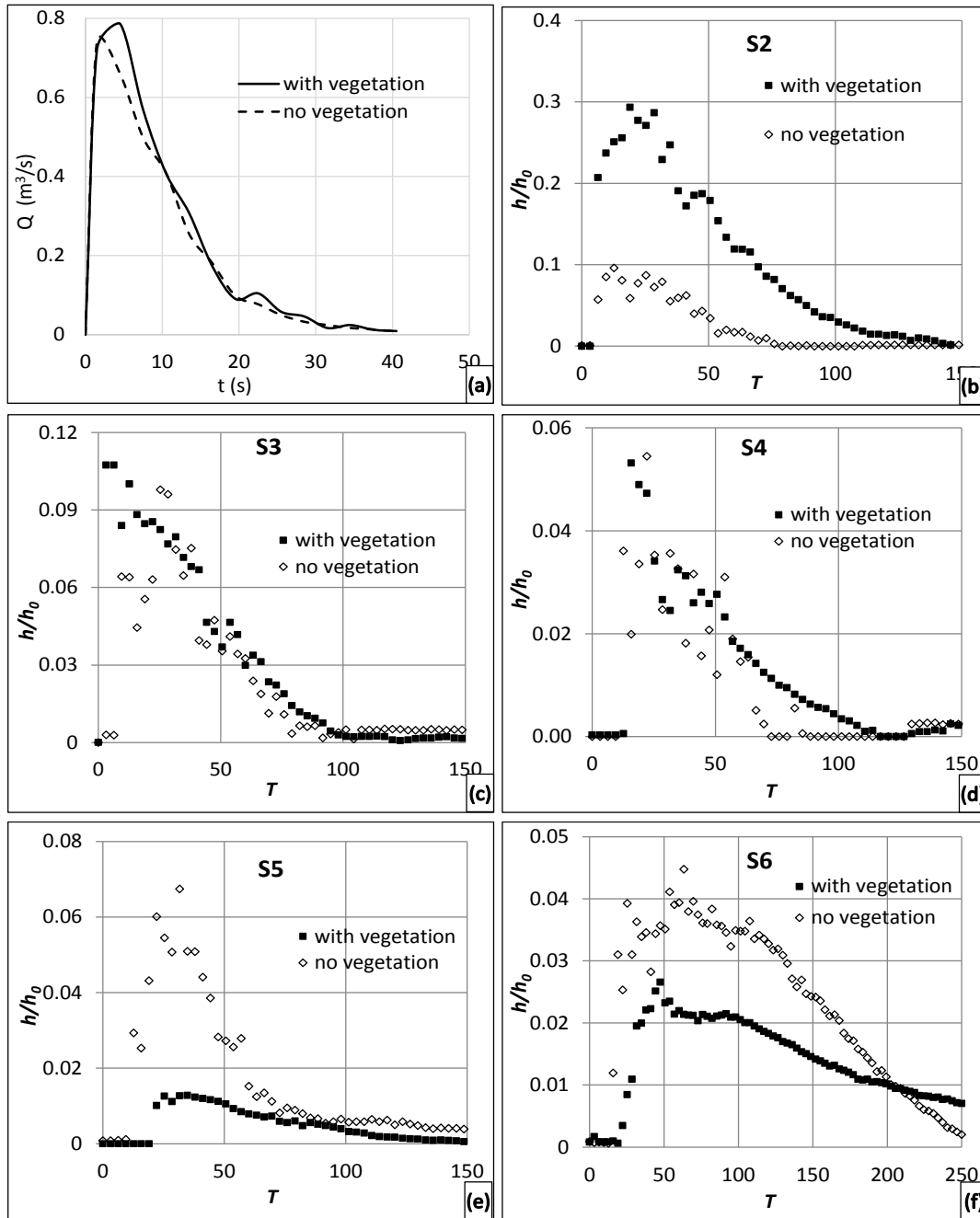


Fig. 4. (a) Output hydrographs $Q(t)$ and dimensionless temporal variation of the water depths h/h_0 for (b) S2 (c) S3 (d) S4 (e) S5 (f) S6 measurement points.

The dam break scenarios were achieved by means of gates of rectangular and triangular shape. The gate was lifted up by a motor and it is opened. The photos of the dam break mechanisms are given in Figure 2.

2.2 Measurements

During the experiments, water levels were measured at six different points and the velocity was measured at one point. The locations and the coordinates of the measurement points are shown in Figure 3.

Temporal variations of water depths were measured by using UltraLab ULS (Ultrasonic level sensor) 80-D device and USS20130 sensors. ULS 80-D has 8 different channels so the

water depths were measured simultaneously from 8 different measurement points. The working range of the USS20130 sensor is between 200 mm and 1300 mm, with a resolution of 0.18 mm. The sample rate and the frequency of the sensor is up to 75 Hz and 200 kHz, respectively.

The temporal velocity values were determined using a SonTek MicroADV to measure water velocity in a wide range of environments such as laboratories, rivers, etc. The sampling rate of the ADV is up to 50Hz and the resolution is 0.01 cm/s. The device sends out a beam of acoustic waves and these waves bounce off moving particulate matter in the water and then calculates the velocity (Tiwari et al., 2016). Kaolin clay was used as suspended solid materials to increase the accuracy of the velocity measurements.

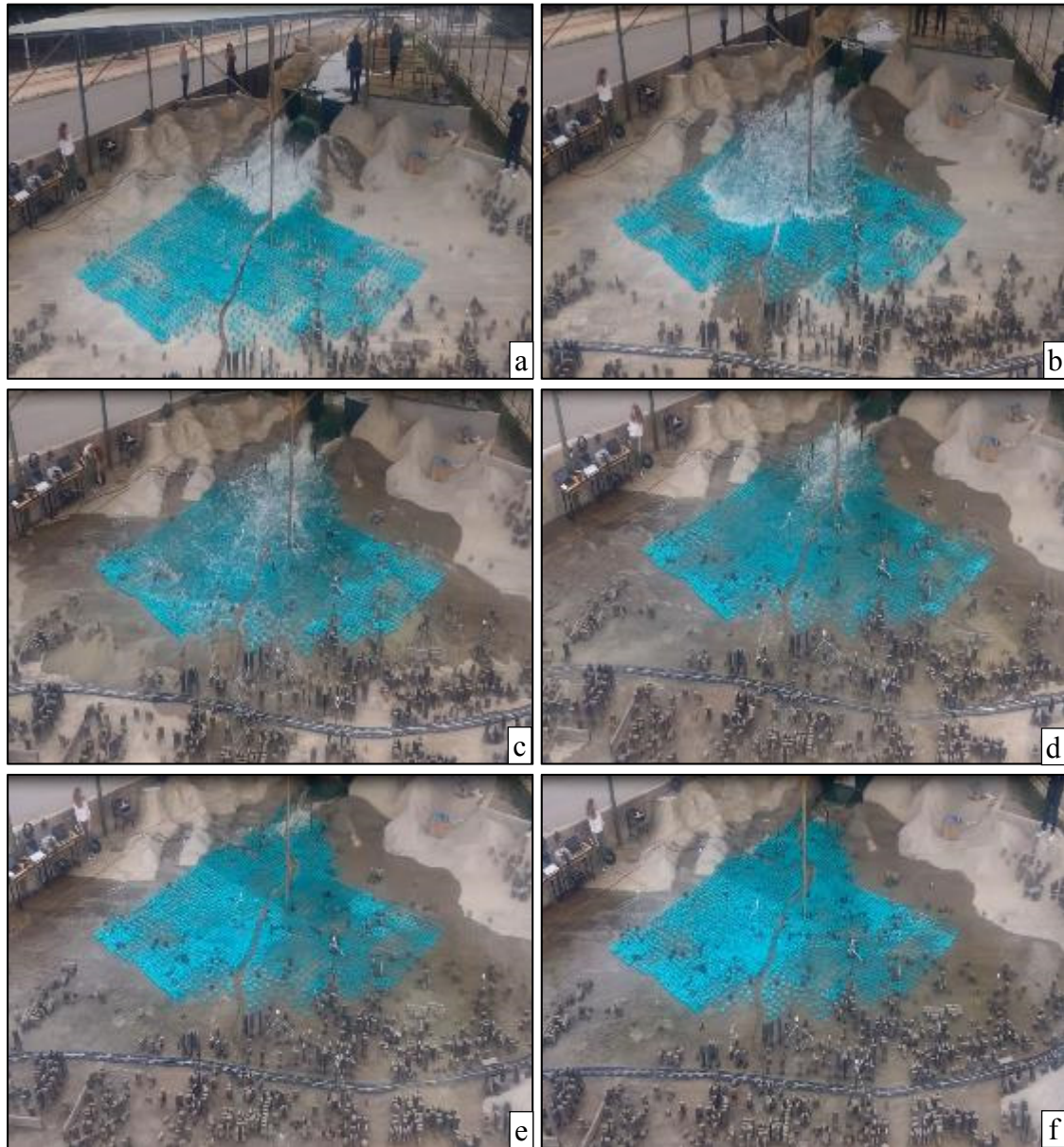


Fig. 5. The images taken at time (a) 3 s, (b) 6 s, (c) 10 s, (d) 15 s, (e) 25 s, and (f) 35 s after gate opening.

3 EXPERIMENTAL RESULTS

Experiments were performed for three different reservoir levels. Since the experiments performed in the case of no vegetation were carried out only for the maximum water level (Tayfur et al., 2013), the results of the present study were compared only for this case. In addition, different reservoir levels were also used in the experiments to investigate the effect of dam reservoir level on flood wave propagation. As a result, six experiments were carried out for three different reservoir levels and two different types of dam failure. Each experiment was repeated at least twice thereby checking the accuracy of the experiments. The output hydrographs related to the experiments were obtained by means of the model reservoir water depth – volume curve. The water depth-volume curve was generated from the calibration performed previously. The experimental results for the no vegetation case were taken from Tayfur et al. (2013).

Since the vertical scale of the distorted dam physical model is $1/30$, the measured water depths are multiplied by 30 to convert to prototype values. The features of experiments performed within the scope of this study are given in Table 2. The output hydrographs and temporal water levels related to the experiment R98 for both vegetation and no vegetation cases are given in Figure 4. To obtain dimensionless water depths, measured water depths were divided into initial reservoir level (h_0). Similarly, dimensionless time (T) obtained by multiplying time (t) with $(g/h_0)^{1/2}$ (Kocaman and Ozmen-Cagatay, 2015) where g is the acceleration of gravity.

According to the results of the vegetated experiment, the water depth increases to around 288 mm at point S2 located on the right bank close to the dam body. This value corresponds to 8.64 m water depth in the prototype. The residential area in this region is sparse and considering the flood wave with a depth of 9 m, it can be said that the first three floors of the buildings will be inundated. This value was 94 mm in the non-vegetated

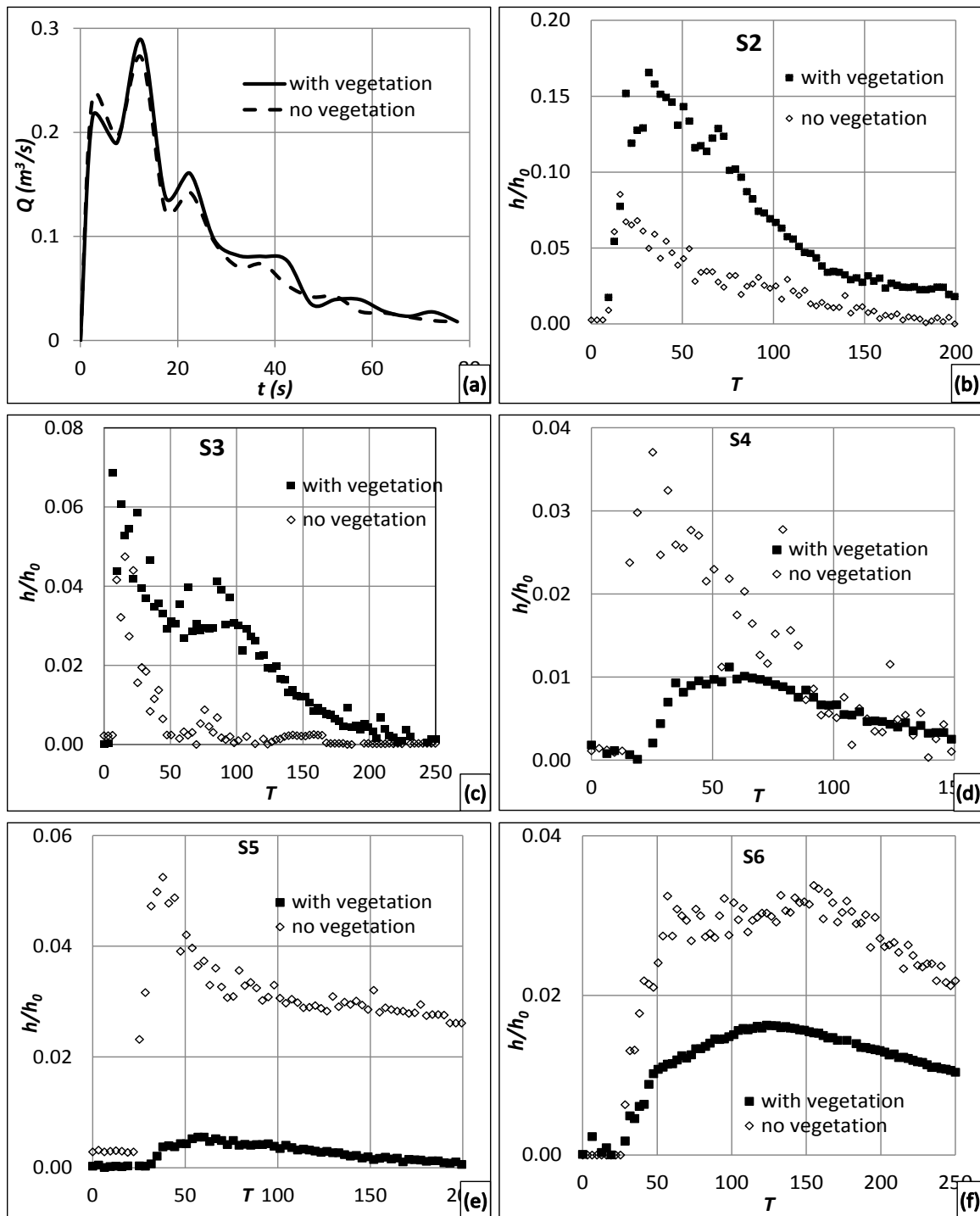


Fig. 6. (a) Output hydrographs $Q(t)$ and dimensionless temporal variation of the water depths h/h_0 for (b) S2, (c) S3, (d) S4, (e) S5, and (f) S6 measurement points.

experiments corresponding to 2.82 m water depth in the prototype. As the vegetation is intensive in this region, the vegetation causes a three-fold increase in water depth. The time for the flood wave to reach this point was measured as 2 seconds in both vegetated and non-vegetated experiments. When this value is transferred to the prototype by using distorted simulation model laws, the flood wave will reach this point in 54.8 s. The time to reach the maximum water level of the flood wave was 4s in the non-vegetated model experiments, while this value was 6 s in the vegetated experiments. These values are 1.83 minutes and 2.74 minutes in the prototype, respectively.

Table 2. The features of the performed experiments.

Experiment No	Type of the dam break	Dam reservoir level (cm)	Vegetation at downstream part
R98	Rectangular	98	Available
R88	Rectangular	88	Available
R80	Rectangular	80	Available
T98	Triangular	98	Available
T88	Triangular	88	Available
T80	Triangular	80	Available



Fig. 7. The images taken at time (a) 3 s, (b) 6 s, (c) 10 s, (d) 15 s, (e) 25 s, and (f) 35 s after gate opening.

The maximum water depths recorded at point S3 on the left bank are similar for vegetated and non-vegetated experiments. Since this measurement point is very close to the dam body, the effect of vegetation is not observed at this point, as predicted.

The level meter S4 is located on the right bank in the middle of the downstream area and close to Urkmez Creek. The measured water depths are very close for vegetated and non-vegetated experiments. The impact time of the flood wave for the vegetated experiment is more than that measured for the non-vegetated experiment.

The point S5 is located in the middle of the downstream area on the right bank and there is settlement area at the downstream part of the measurement point. The presence of vegetation causes a significant decrease in the water depth as the flood wave propagates to the downstream and greatly reduces its impact on the settlements. The presence of vegetation not only reduced the depth of the flood wave, but also provided a significant delay in reaching this point.

The S6 level meter is located in the middle part of the downstream area on the left bank. In this region where the settlement

area is more intense there was a decrease in the maximum water depth due to vegetation.

The images taken at 3 s, 6 s, 10 s, 15 s, 25 s, and 35 s after the rectangular gate is opened are given in Figure 5.

The output hydrographs and temporal water levels related to the experiment no T98 for both vegetation and absent vegetation cases are given in Figure 6.

The results obtained for triangular collapse are similar to those obtained for rectangular collapse. The vegetation causes a two-fold increase in water depth at point S2 where the vegetation is intensive. At point S3, the effective duration of the flood wave in the vegetated case is more than the non-vegetated case. At points S4 and S5 the presence of vegetation causes a significant decrease in the water depth as the flood wave propagates to the downstream and greatly reduces its impact on the settlements. The presence of vegetation not only reduced the water depth of the flood wave, but also provided a significant delay in reaching these points. At point S6 where the settlement area is more intense there was a decrease in the maximum water depth due to vegetation.

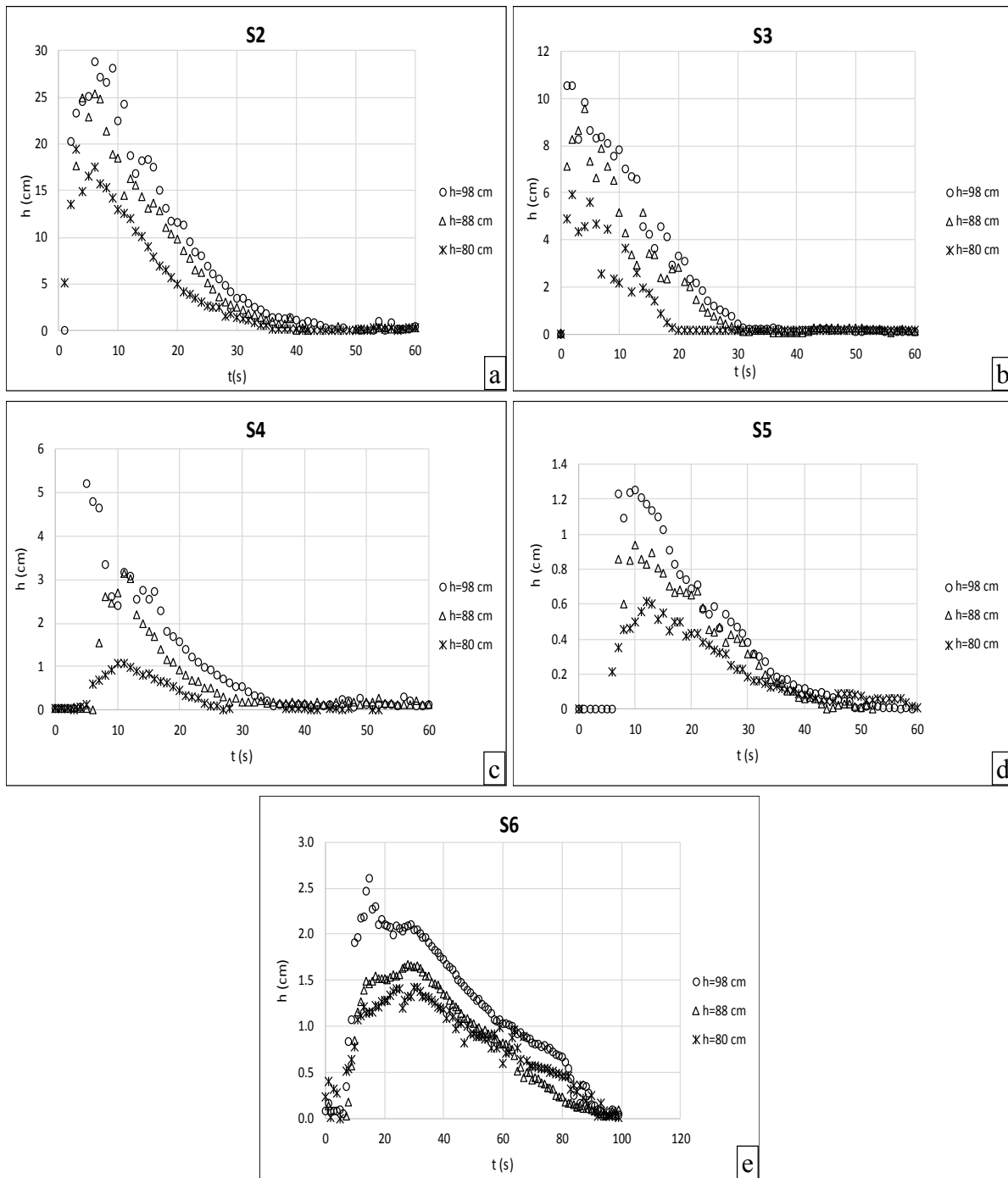


Fig. 8. The comparison of the temporal water levels related to the rectangular collapse experiments R98, R88 and R80 for a) S2, b) S3, c) S4, d) S5, and e) S6.

The images taken at 3 s, 6 s, 10 s, 15 s, 25 s, and 35 s after the triangular gate is opened are given in Figure 7. The temporal propagations of the flood waves differ between the rectangular and triangular collapses, and in the case of a triangular collapse this propagation is slower than the rectangular one.

The vegetated experiments were also carried out for three different reservoir levels to investigate the effect of dam reservoir level on flood wave propagation. The comparison of the temporal water levels measured for rectangular and triangular collapses are given in Figure 8 and Figure 9, respectively.

According to the results of the experiments, it is revealed that as the reservoir level decreases, the water depths measured

during the propagation of the flood wave in the downstream region decrease and the time to reach the maximum water depth increases. This expected result also proves the accuracy of the performed experiments and can be used for numerical researches during the calibration process. The results obtained from different reservoir levels also show that the duration of the flood wave is independent of dam reservoir level.

Time dependent velocities for rectangular and triangular collapse types are given in Figure 10 and Figure 11, respectively. The velocity measurement point (V) is located close to measurement point S2.

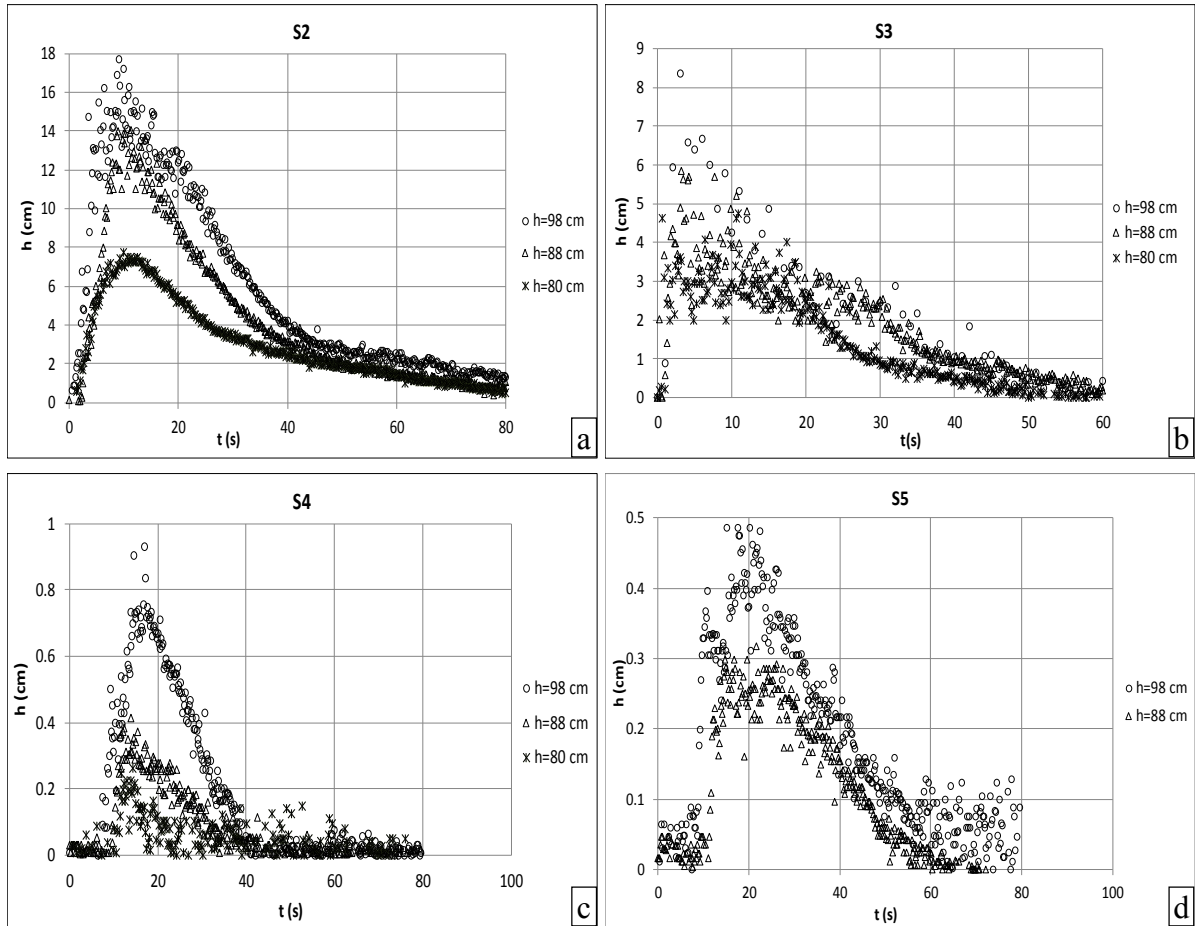


Fig. 9. The comparison of the temporal water levels related to the triangular collapse experiments T98, T88 and T80 for a) S2, b) S3, c) S4, and d) S5.

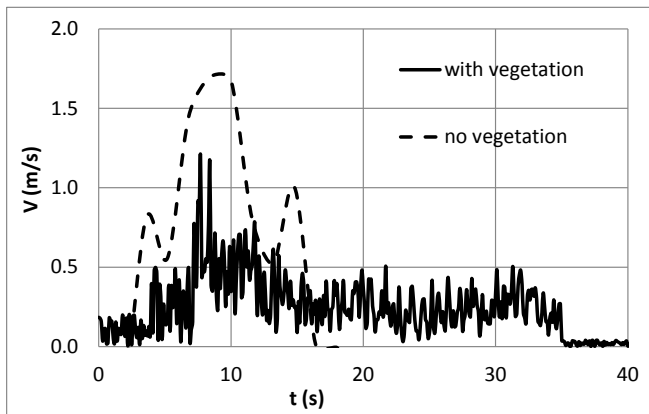


Fig. 10. Temporal variations of the velocity measured at point V for rectangular collapse type.

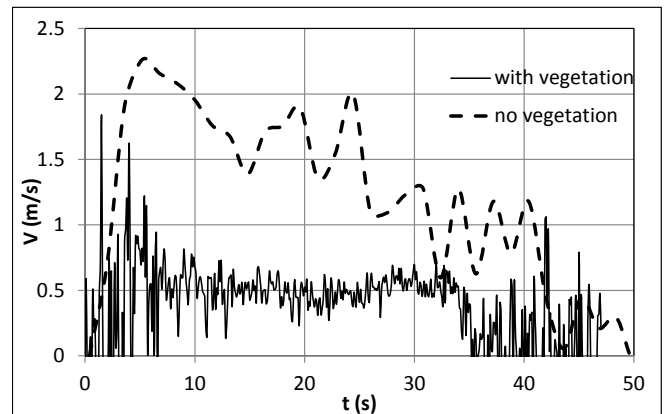


Fig. 11. Temporal variations of the velocity measured at point V for triangular collapse type.

In the vegetated experiment, the maximum velocity was measured at around 1.2 m s^{-1} and 1.5 m s^{-1} for rectangular and triangular collapse types, respectively. These values were measured as 1.7 m s^{-1} and 2.2 m s^{-1} for the non-vegetated experiments. In vegetated experiments, the maximum velocity values correspond to 6.58 m s^{-1} and 8.22 m s^{-1} in the prototype for rectangular and triangular collapse types, respectively, while these values are 36.05 m s^{-1} and 45.04 m s^{-1} for the non-vegetated case. As shown by these values, the presence of the vegetation induced a significant decrease in velocity values.

The measured maximum velocity value for triangular collapse is greater than that measured for rectangular collapse. The main reason is that vegetation causes a further increase in water depth in the case of rectangular collapse. The water level increases by 206% for rectangular collapse, while this ratio is 94% for triangular collapse. Measured maximum water depths for each measurement point and time to reach of the flood wave to the measurement points for vegetated and absent vegetated cases are given in Figure 12.

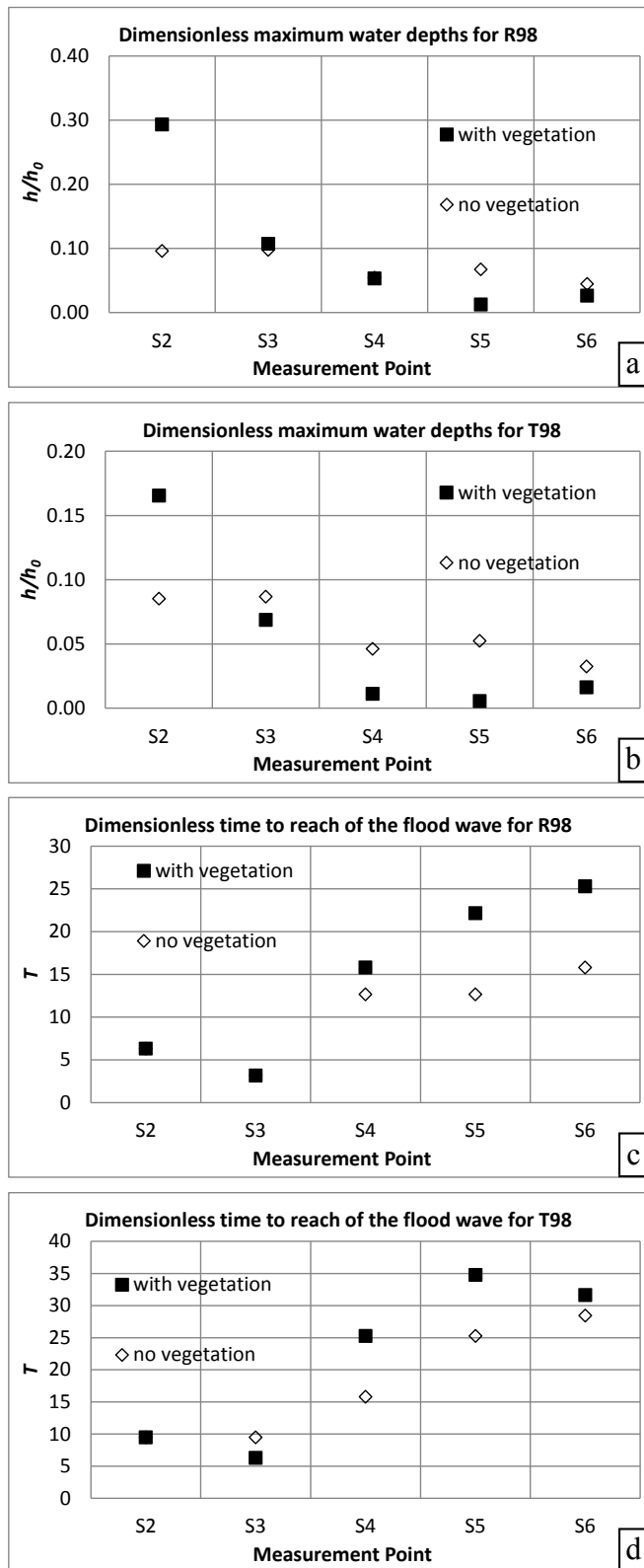


Fig. 12. Measured maximum water depths for each measurement point and time for the flood wave to reach the measurement points. a) Dimensionless maximum water depths for R98 b) Dimensionless maximum water depths for T98 c) Dimensionless time for the flood wave to reach R98 d) Dimensionless time for the flood wave to reach T98.

As shown in Figure 12, the vegetation causes a three-fold increase in water depth at S2, which is located where the vegeta-

tion is intensive. The effect of vegetation on the maximum water depth is not observed at point S3 since the location of this point is very close to the dam body. The time required for the flood wave to reach the points S2 and S3 is almost the same for both vegetated and non-vegetated experiments. In the vegetated experiments, the flood wave reaches the points S4, S5 and S6 (where settlement area is intense) both in less depth and in more time. In the case of rectangular collapse, the water levels decrease by 2.4%, 81.2% and 40.8% for points S4, S5 and S6, respectively, while these rates are 75.7%, 89.5% and 50% in the case of triangular collapse. Therefore, the presence of vegetation significantly reduces the effects of the flood wave in settlements. The vegetation also caused the mitigation of the flood wave and so its effect decreased through the downstream part of the studied area.

4 CONCLUSIONS

The effects of vegetation on the flood wave propagation for two different dam break shapes and three different reservoir levels were investigated experimentally by using the distorted physical model of Urkmez Dam Lake and its downstream residential area. According to the experimental results, the following conclusions can be drawn:

- The vegetation causes about two or three times higher water depths than those of no vegetation case near the dam body where the vegetation exists intensively.
- The presence of vegetation causes a significant decrease in the water depth as the flood wave propagates to the downstream and greatly reduces its impact on the settlements. The presence of vegetation not only reduced the depth of the flood wave, but also provided a significant delay in reaching downstream part of the studied area.
- As the reservoir level decreases, the water depths measured during the propagation of the flood wave in the downstream region decrease and the time to reach the maximum water depth increases. This expected result also proves the accuracy of the performed experiments and can be used for numerical researches during the calibration process and different scenarios can be simulated numerically.
- The vegetation causes a further reduction in the impact of flood wave propagation in the case of triangular collapse. In other words, flood wave propagation does not only depend on the vegetation itself but also the dam break shape, hence the resulting outflow hydrograph.
- Dam break shape plays a more important role in the temporal variation of the flood wave than the presence of vegetation.
- Considering that the triangular collapse situation is more realistic in nature, the presence of vegetation downstream of dams causes a significant reduction in the devastating effects of the flood wave.

It should be noted that experimental studies have several limitations such as characteristics of design or methodology. Therefore, numerical modeling studies are required to further investigation of the effects of vegetation on the flood wave propagation in case of dam break. However, the results obtained from physical model experiments may be useful for initiating the design of vegetated downstream areas and for calibration of numerical models.

Acknowledgements. The authors thank to the Scientific and Technological Research Council of Turkey (TUBITAK) for supporting the study through the project 116M237.

REFERENCES

- Elkholy, M., Larocque, L.A., Chaudhry, M.H., Imran, J., 2016. Experimental investigations of partial-breach dam-break flows. *J. Hydraul. Eng.*, 142, 1–12. [https://doi.org/10.1061/\(ASCE\)HY.1943-7900.0001185](https://doi.org/10.1061/(ASCE)HY.1943-7900.0001185)
- Ferrari, A., Fraccarollo, L., Dumbser, M., Toro, E.F., Armanini, A., 2010. Three-dimensional flow evolution after a dam break. *J. Fluid Mech.*, 663, 456–477. <https://doi.org/10.1017/S0022112010003599>
- Güney, M.S., Tayfur, G., Bombar, G., Elci, S., 2014. Distorted physical model to study sudden partial dam break flows in an urban area. *J. Hydraul. Eng.*, 140, 05014006. [https://doi.org/10.1061/\(ASCE\)HY.1943-7900.0000926](https://doi.org/10.1061/(ASCE)HY.1943-7900.0000926)
- Haltas, I., Tayfur, G., Elci, S., 2016. Two-dimensional numerical modeling of flood wave propagation in an urban area due to Ürkmez dam-break, İzmir, Turkey. *Nat. Hazards*, 81, 2103–2119. <https://doi.org/10.1007/s11069-016-2175-6>
- He, Z., Wu, T., Weng, H., Hu, P., Wu, G., 2017. Numerical simulation of dam-break flow and bed change considering the vegetation effects. *Int. J. Sediment Res.*, 32, 105–120. <https://doi.org/10.1016/j.ijsrc.2015.04.004>
- Hooshyaripor, F., Tahershamsi, A., Razi, S., 2017. Dam break flood wave under different reservoir's capacities and lengths. *Sadhana - Acad. Proc. Eng. Sci.*, 42, 1557–1569. <https://doi.org/10.1007/s12046-017-0693-x>
- Ismail, H., Abd Wahab, A.K., Alias, N.E., 2012. Determination of mangrove forest performance in reducing tsunami run-up using physical models. *Nat. Hazards*, 63, 939–963. <https://doi.org/10.1007/s11069-012-0200-y>
- Kocaman, S., Ozmen-Cagatay, H., 2015. Investigation of dam-break induced shock waves impact on a vertical wall. *J. Hydrol.*, 525, 1–12. <https://doi.org/10.1016/j.jhydrol.2015.03.040>
- LaRocque, L.A., Imran, J., Chaudhry, M.H., 2013. Experimental and numerical investigations of two-dimensional dam-break flows. *J. Hydraul. Eng.*, 139, 569–579. [https://doi.org/10.1061/\(asce\)hy.1943-7900.0000705](https://doi.org/10.1061/(asce)hy.1943-7900.0000705)
- Lauber, G., Hager, W.H., 1998. Experiments to dambreak wave: Horizontal channel. *J. Hydraul. Res.*, 36, 291–307. <https://doi.org/10.1080/00221689809498620>
- Liu, L., Sun, J., Lin, B., Lu, L., 2018. Building performance in dam-break flow—an experimental study. *Urban Water J.*, 15, 251–258. <https://doi.org/10.1080/1573062X.2018.1433862>
- Ozmen-Cagatay, H., Kocaman, S., 2010. Dam-break flows during initial stage using SWE and RANS approaches. *J. Hydraul. Res.*, 48, 603–611. <https://doi.org/10.1080/00221686.2010.507342>
- Ozmen-Cagatay, H., Kocaman, S., Guzel, H., 2014. Investigation of dam-break flood waves in a dry channel with a hump. *J. Hydro-Environment Res.*, 8, 304–315. <https://doi.org/10.1016/j.jher.2014.01.005>
- Soares-Frazão, S., 2007. Experiments of dam-break wave over a triangular bottom sill. *J. Hydraul. Res.*, 45, 19–26. <https://doi.org/10.1080/00221686.2007.9521829>
- Soares-Frazão, S., Zech, Y., 2008. Dam-break flow through an idealised city. *J. Hydraul. Res.*, 46, 648–658. <https://doi.org/10.3826/jhr.2008.3164>
- Tayfur, G., Güney, M.Ş., Haltas, İ., Elçi, Ş., Bombar, G., 2013. Experimental and Numerical Investigation of Dam Break Floods - GIS Applications for Dams. TUBITAK Project No : 110M240 (Final Report). (In Turkish.)
- Tiwari, H., Khan, A., Sharma, N., 2016. Emerging methodologies for turbulence characterization in river dynamics study. In: Sharma, N. (Ed.): *River System Analysis and Management*. Springer, pp. 167–186. ISBN: 9811014728. ISBN: 9789811014727.
- Zhang, M.L., Xu, Y.Y., Qiao, Y., Jiang, H.Z., Zhang, Z.Z., Zhang, G.S., 2016. Numerical simulation of flow and bed morphology in the case of dam break floods with vegetation effect. *J. Hydrodyn.*, 28, 23–32. [https://doi.org/10.1016/S1001-6058\(16\)60604-2](https://doi.org/10.1016/S1001-6058(16)60604-2)
- Zhang, T., Fang, F., Feng, P., 2017. Simulation of dam/levee-break hydrodynamics with a three-dimensional implicit unstructured-mesh finite element model. *Environ. Fluid Mech.*, 17, 959–979. <https://doi.org/10.1007/s10652-017-9530-3>

Received 7 May 2020

Accepted 1 July 2020